J Biochem Tech (2018) Special Issue (2): 1-8
ISSN: 0974-2328

Enhanced Ammonia Gas Sensing Properties Using Polyaniline/Na-doped ZnO Nanowires at Room Temperature toward Biomedical Sensor Application

Abdolhossein Sa'aedi , Pejman Shabani* and Ramin Yousefi

Received: 24 March 2018 / Received in revised form: 01 June 2018, Accepted: 02 June 2018, Published online: 05 September 2018

Abstract

In the present work, a comparative study of gas sensor performance of pristine polyaniline (PANI), PANI/ZnO nanowires, and PANI/Na-doped ZnO nanowires heterostructure to ammonia was carried out in room temperature. The PANI/Na-doped ZnO nanowires showed excellent gas-sensing performance against ammonia in comparison with the other samples. Moreover, the response and recovery time of the PANI/Na-doped ZnO nanowires were shorter than those of the other samples. Furthermore, PANI/ZnO nanowires ZnO nanowires performed good selectivity compared to the other samples, therefore it's can be used as a biosensor. In fact, the protonation and deprotonation process of PANI/ZnO plays essential role in the enhancement of the gas sensing performance.

Keywords: PANI/ZnO nanowires, Gas sensing, Thermal evaporation method, Protonation and deprotonation.

Introduction

Ammonia is a colorless toxic gas with a pungent odor, that is produced in industries such as chemical production, organic chemical manufacturing, refrigeration and so on. The detection of NH_3 is quite necessary because breathing lower concentrations of ammonia can cause coughing, wheezing, laryngitis, fever, nausea, pink frothy phlegm and exposure to extremely high levels of ammonia can cause death or lung damage, collapse (Wang et al., 2017; Nguyen et al., 2015). Among different metal oxide nanostructures, ZnO has been selected as a gas sensing due to its unique properties. ZnO is an n-type semiconductor with a wide band gap (3.3 eV) at room temperature. In addition, introducing a doping material in ZnO structure during the growth and synthesis process is straightforward by a simple growth method such as thermal evaporation method which is one of the common methods of growing ZnO nanostructures for different applications (Tian et al., 2017; Hwang et al., 2012).In contrast to these advantages; it has a major disadvantage for gas sensing application, which is its high working temperature. We recently reported gas-sensing applications of group-I-doped ZnO nanorods and it has been showed that Na as a doping material could decrease working temperature of ZnO gas sensor (Sa'aedi &. Yousefi, 2017). However, this decreasing was not significant. Therefore, another strategy should be presented to decrease working temperature of ZnO gas sensor device. In addition, recently, heterostructures of metal-oxide and organic semiconducting polymers are the best candidates for fabrication gas sensing device at room temperature (Zhu et al., 2016; Bai et al., 2017; Xu et al., 2016; Das, & Sarkar, 2017; Dhawale et al., 2010; Bandgar et al., 2017). Therefore, it is expected that, group-I-doped ZnO/organic semiconducting heterostructures can be a good candidate for fabrication of gas sensing device that is working in lower temperature (RT) in compared to working temperature of the pristine ZnO nanostructures. Among different organic semiconductor, polyaniline (PANI) is the best candidate for gas sensing applications due its unique properties such as unique conductivity property, chemical stability in the environment, and tunable optical and electrical properties (Steffens et al., 2012; Tai et al., 2008).

According to above reasons, in the present work, undoped and Na-doped ZnO nanowires/PANI heterostructures were grown as gas sensors devices that were worked in RT. To the best of our knowledge, a comparative study about gas-sensing performance of the undoped ZnO/PANI and Na-doped ZnO/PANI nanowires has not been reported yet.

Abdolhossein Sa'aedi and Pejman Shabani*

Department of Electrical Engineering, Mahshahr Branch, Islamic Azad University (I.A.U), Mahshahr, Iran.

Ramin Yousefi

Department of Physics, Masjed-Soleiman Branch, Islamic Azad University (I.A.U), Masjed-Soleiman, Iran.

***Email:** p.shabani2017@yahoo.com

Experiments

Growth of undoped and doped ZnO nanowires

In the first step, undoped & Na-doped ZnO NWs were grown on Si/SiO_2 substrates, which the experimental details and some characterization were reported in our previous work (Sa´aedi et

al., 2014). Si (100) wafers were employed as substrates, which were cleaned by a standard process. After cleaning the Si substrates, a thick oxide layer was formed on the substrates by annealing the substrates under oxygen ambient in a furnace under 700 °C. A mixture of zinc oxide powder (99.99%) and graphite powder in a 1:1 weight ratio was used to grow undoped ZnO NWs and zinc oxide powder, NaOH powder, and commercial graphite powder in a 10:1:10 weight ratios was used as the precursor material to grow the Na-doped ZnO NWs. The small tube was then inserted into the vacuum chamber so that the closed end was at the center of the furnace. The source material was heated up to 950 ºC and the temperature of the substrate was maintained at 600 ºC during growth. High purity nitrogen gas was fed at about 200 Sccm into the furnace at one end, while the other end was connected to a rotary pump. The growth process was allowed to proceed for 1 h. A vacuum of 50 Torr was maintained inside the tube furnace during the deposition of the nanostructures. According to these conditions, two sets of the undoped and Na-doped ZnO NWs were grown.

Synthesis of polyaniline and PANI/ZnO nanocomposites

Materials, methods, and steps, which were used to synthesize PANI, are shown schematically in Fig. 1. After papering the PANI, a layer of the PANI was deposited on ZnO NWs films by a spin coating method under low magnetic fieled (0.1 T). Then, the films were dried on hotplate at 70 °C during 30 min

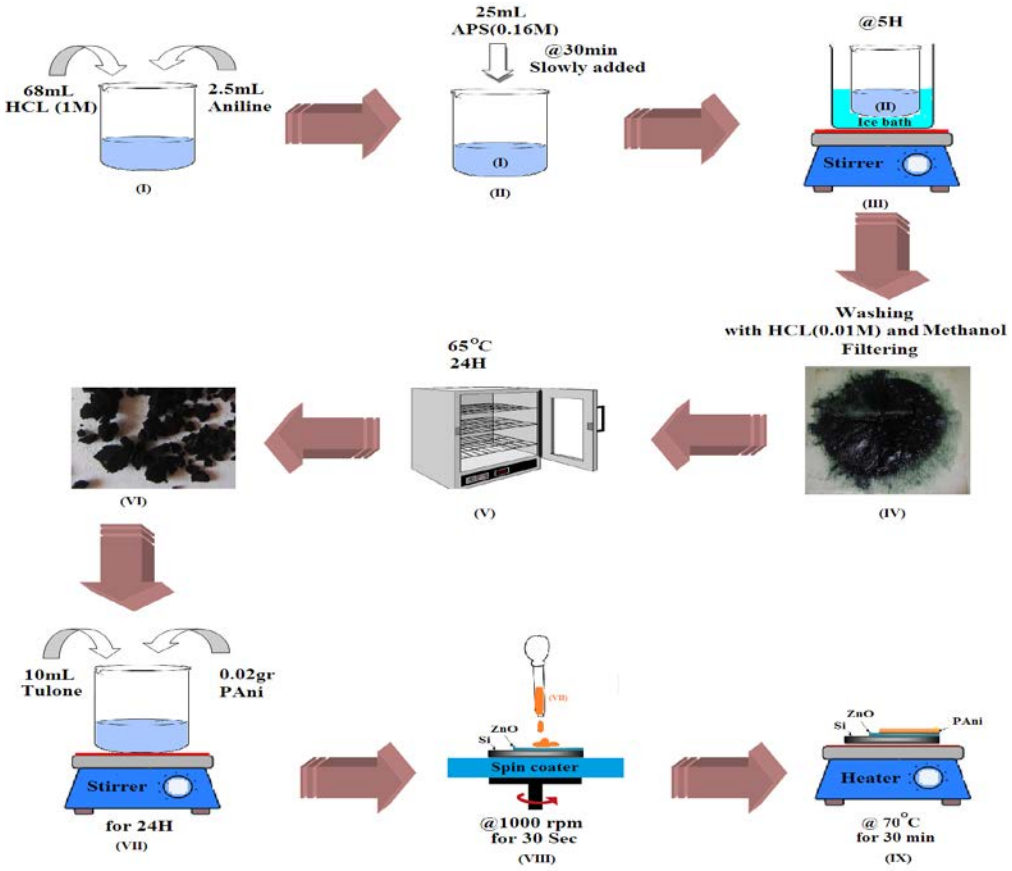

Figure 1. Schematic diagram to synthesize PANI.

Characterization

The resulting samples were characterized, using several tools to check their quality. The crystal phase and morphology of the products were characterized by an X-ray powder diffractometer (XRD, Philips, X'pert, system using CuK$_\alpha$ radiation) and a field emission electron microscope (FESEM, Quanta 200F). The elemental contents of the products were investigated via X-ray photoelectron spectra (XPS) (VG-Microtech ESCA-2000 with MgKα radiation as the excitation source) in our previous work (Tai et al., 2008).

Fabrication and measurement of the gas sensor

Detailed gas sensing fabrication and measurements is similar with our previous work that was shown schematically in Fig. 2(Sa'aedi & Yousefi, 2017). First, the samples were put into the test chamber. Next, the resistance of the samples was measured to ensure a stable condition; additionally, a calculated amount of the target gas, which was controlled by a gas flow meter, was introduced to the set-up chamber, which its relative humidity was controlled. At this time, the resistance value of the samples changed, which was measured by a digital multimeter (Fig. 2).

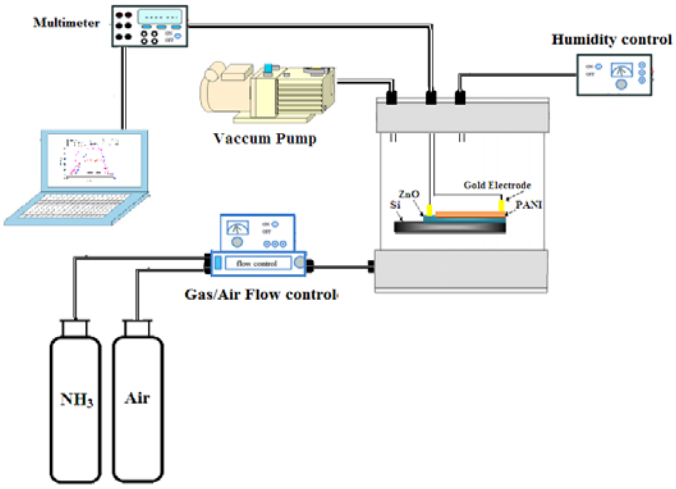

Figure 2. Schematic of our gas sensor set-up.

$S=R_g/R_a$ was defined as the response of the sensors, where R_a is the sample resistance in air, and R_g is the sample resistance when the samples were exposed to target gases. The humidity of the chamber was measured by a humidity controller and was kept constant during the measurements. The response time (t_{res}) was considered as the time when the sample resistance reached 90% of the equilibrium value after introducing gas to the set-up chamber. The recovery time (t_{rec}) was considered as the time when the sample resistance returned to 10% above the initial value in air after releasing the target gas. MQ-3 gas sensing device (Hanwei Electronic CO. LTD) was used for calibration of the fabricated gas sensor device in current work.

Results and Discussion

Morphology, structure, and optical studies of the samples

Figs. 3(a) and (b) show the FESEM images of the undoped and Na-doped ZnO NWs, respectively. As can be observed in this FESEM image, the undoped ZnO NWs were randomly grown on the Si substrate, with a uniform diameter of approximately 80 nm and length of several hundred micrometers. Fig. 3 (b) shows an FESEM image of the Na-doped ZnO samples that have an average length of several hundred nanometers and they are like a rode shape with an average diameter of approximately 60 nm. In fact, Na as a passivation agent caused decrease growth rate. Therefore, under the same conditions, the Na-doped ZnO NWs length and average diameter are smaller than undoped NWs length and average diameter(Huang, & Wang, 2009). Also the aspect ratio of doped ZnO was higher than undoped ZnO, which is - important because it can be effective in improvement of gas sensing response of hybrid film base sensors by increasing in diffusion of gas molecules into the structures (Zhu et al., 2016).

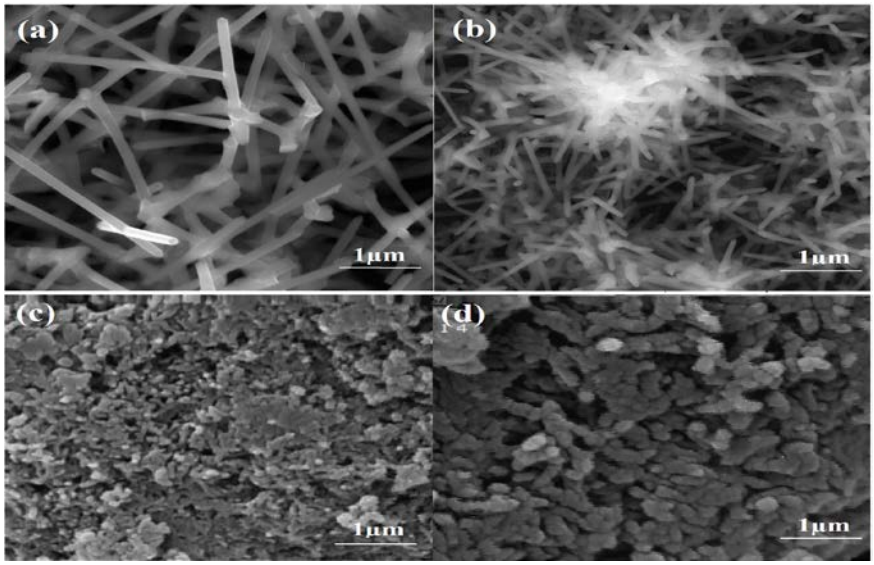

Figure 3. FESEM image of (a) undoped ZnO NWs, (b) Na-doped ZnO NWs, (c) PANI/ZnO nanocomposites layer, and (d) PANI/Na-doped ZnO nanocomposites layer.

The XRD patterns of the samples are shown in Fig. 4. These patterns indicated a hexagonal wurtzite structure for the undoped and doped ZnO NWs, which is in a good agreement with the bulk ZnO structure with the card number of JCPDS No. 80-0075. No peaks from Na_2O or other impurities are visible. In addition, the XRD peaks of the doped samples showed a slightly shift toward lower angles in comparison with the undoped ZnO (is not shown here), that could be due to bigger ionic radii of Na^+ (1.02 Å) than ionic radius of Zn^{2+} (74 Å). Furthermore, the full width at half maximum (FWHM) of the XRD peaks of doped samples is bigger than that of the undoped sample leading to the lower crystallite size in these samples. Such a result demonstrates that the crystalline quality of the doped samples is lower than that of the undoped samples, and the optical properties of the doped samples can be affected by this lower crystalline quality. In addition, XRD pattern of the pristine PANI is shown in Fig. 4. This pattern indicates that, the PANI sample is crystallinity and it can be played as a semiconducting material.

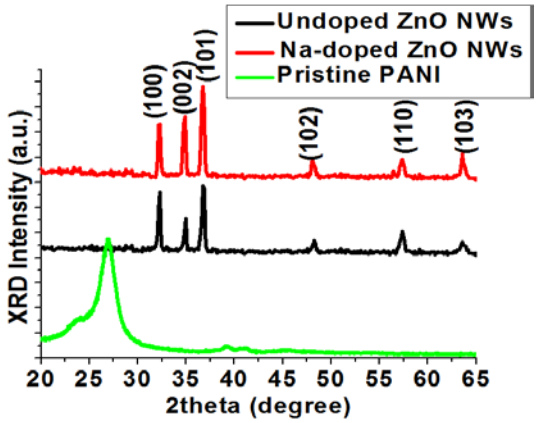

Figure 4. XRD patterns of the undopedand Na-doped ZnO NWs and pristine PANI.

According to the our previous works, Na as a doping material caused increase oxygen vacancy in ZnO structure that could be due to big difference between zinc and sodium ionic radii (Sa'aedi &. Yousefi, 217; Sa´aedi et al., 2014). Thus, the XPS result of O 1s demonstrates that Na-doped ZnO NWs possesses oxygen vacancies. Fig. 5(a) shows the asymmetric N 1s core level of pristine PANI. It can be seen, the peak was deconvoluted to three peaks that are corresponding separately to N in benzenoid amine (–NH–), radical nitrogen cations(═$NH^{\bullet+}$=) and in cationic nitrogen (–NH^{2+}–) structures (Zhou et al.,2014), and the area ratios of the three peaks for the pristine PANI are 69.24%, 19.17%, and 11.59%. Fig. 5(b) and (c) reveal N 1s of PANI layers that were deposited on the undoped ZnO NWs and Na-doped ZnO NWs. As can be seen, feature of N 1s peaks were changed in compared to the N 1s peak of the pristine PANI, which could be due to interaction of the PANI and NWs. These peaks were also deconvoluted to three peaks. However, area ratios of the peaks in these samples are different in compared to the pristine PANI. It can be clearly seen that the totally area from protonated nitrogen atoms of PANI, ZnO/PAni and ZnO:Na/PAni are 30.7%, 46.51% and 61.45%, respectively. This means that Na doped ZnO/PANI heterostructure may has a significantly higher level of protonation (Kulkarni et al., 2017). In fact such different feature of N 1s peaks could be due to electron transfer between PANI and the NWs. However, the oxygen vacancy concentration is different for two NWs that caused change electron transfer rate between PANI and the NWs (Bai et al., 2017). Therefore, N 1s peak feature of two NWs samples is also different.

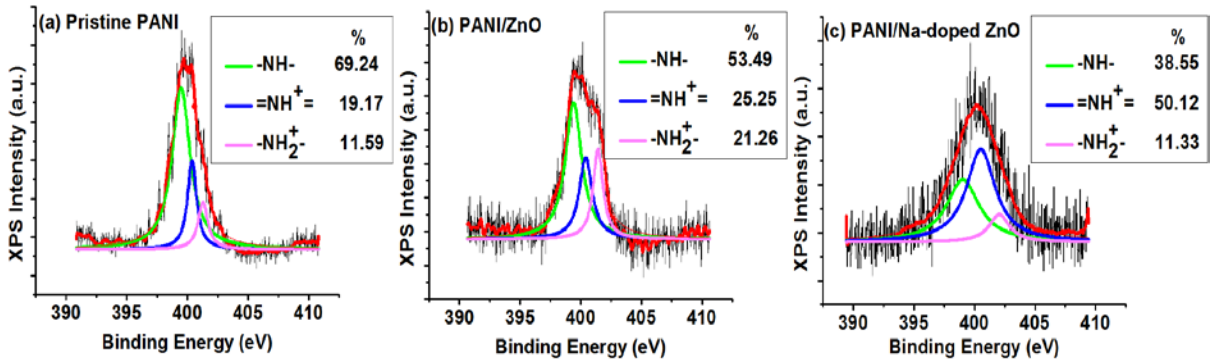

Figure 5. XPS spectrum of N 1s orbital of (a) pristine PANI, (b) PANI/ZnO layer nanocomposite, and (c) PANI/Na-doped ZnO layer nanocomposite.

Gas-sensing measurements

To understand the enhanced gas-sensing performance of the pristine PANI, PANI/ZnOnanocomposite layer, and PANI/Na-doped ZnO nanocomposite layer, first the resistance of the films was measured before and after the exposition of the films to gas by a dynamic response characteristic of the films under 100 ppm ammonia concentration expositions. Resistance change curves of the samples for 100 ppm ammonia concentrations are indicated in Fig. 6 (a). It is crystal clear that the resistance of the samples

increases rapidly by ammonia exposition. As can be observed, response and recovery time are different for the samples, and PANI/ZnO nanocomposite layer exhibits faster response and shorter recovery time compared to the other films. In addition, Fig. 6(b) shows response of the films to different concentration of ammonia gas. It can be seen, the PANI/ZnO layers can detect ammonia gas in low concentration, while, it cannot be seen any response from the pristine PANI in these concentrations.

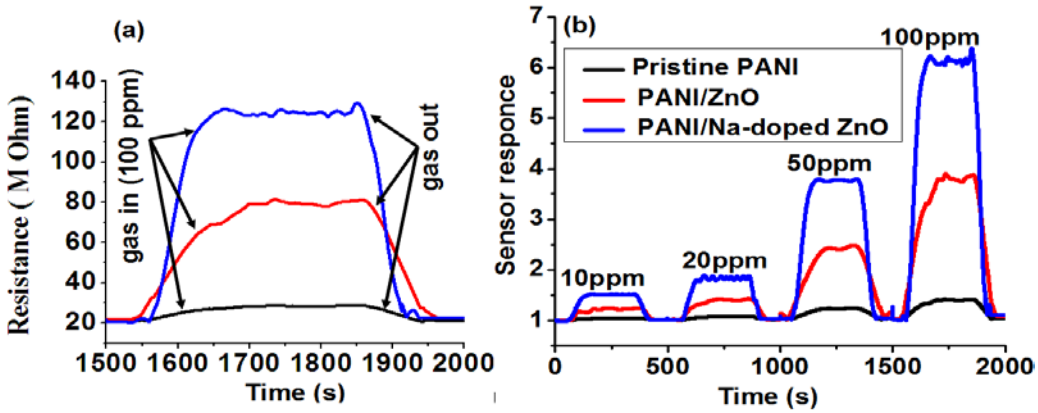

Figure 6. (a) The enlarged response and recovery transients of the undoped and doped samples to 100 ppm ammonia (b) Resistance change curves of the undoped and doped samples toward different ammonia concentrations in dynamic conditions.

Fig.7(a) shows the response of the sample sensors sequentially exposed to 2, 5, 10, 25, 50, 100, and 200 ppm ammoniaat room temperature. The response of the sensors increases by increasing the ammonia concentrations. However, the response of PANI/Na-doped ZnO layer is higherin all concentrations of ammoniagas. The sensor response can be empirically represented as(Patil et al., 2012):

$$S = \frac{{}^{R_g}/_{R_0}}{C_g} \qquad (1)$$

Where C_g is gas concentration (NH_3), R_g and R_0 are resistance of the films under gas exposition and air conditions, respectively. Slope represents the S of tested devices. r^2 represents the linearity of the curves fitting.Sensitive properties of pristine PANI film, PANI/ZnO layer, and PANI/Na-doped ZnO layer nanocomposites to NH_3 are demonstrated in Fig.7(b). It can be seen, sensitivities of the tested sensors are 5×10^{-3}, 31×10^{-3}, and 60×10^{-3} ppm^{-1} for the pristine PANI, PANI/ZnO layer, and PANI/Na-doped ZnO layernanocomposites, respectively. This dramatic increase of slope is attributed to the porous structures of PANI and interface behavior of PANI and Na-doped ZnO NWs, where more sites for gas adsorption in the hybrid film is available compared with pristine PANI film. There is a noteworthy feature that all r^2 of the fitting curves is above 0.95, implying a good linearity in the test concentration region.

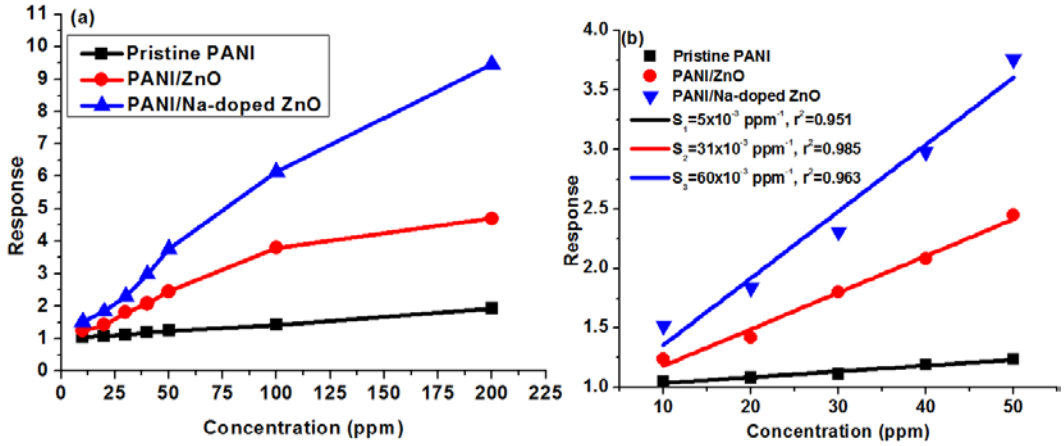

Figure 7. (a) Response curves of the undoped and PANI/ZnO nanowires ZnOnanowires for different ammonia concentrations. (b) Enlarged response curves.

One of the important factors in practical applications of a sensor is to ensure its accuracy and stability during a long time. Hence, we measured the responses of the samples to 100 ppm ammonia in a two-month period. As depicted in Fig.8, PANI/Na-doped ZnO layer nanocompositeexhibits a long-term stability and constant response to 100 ppm ammonia, approximately. Consequently, these sensors could be applied to monitor ammonia in a practical condition.

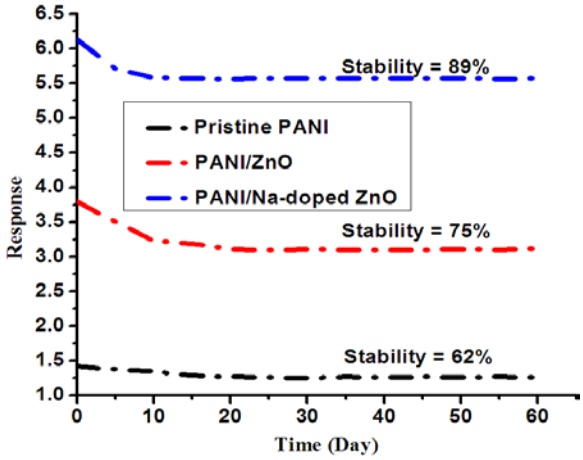

Figure 8. Long-time stability of the pristine PANI, and PANI/ZnO nanowires to 100 ppm ammonia.

In addition, the selectivity of the samples was studied at the corresponding optimal temperatures of all samples by exposing the sensors to several reducing gases such as 100 ppm of ethanol (C_2H_5OH), liquid petroleum gas (LPG), carbon monoxide (CO), ammonia (NH_3), and methanol (CH_3OH). Indeed, selectivity is one of the key parameters for gas-sensitive materials and is affected by many factors such as morphology, crystalline structure, and doping(Sengupta et al., 2009). The selectivity of the samples is shown in Fig. 9. As a result, the PANI/Na-doped ZnO layer nanocomposite displays a higher response to these gases in comparison with the pristine PANI and PANI/ZnO layer nanocomposite. This highly selectivity is caused by best Ammonia intermolecular interaction -based on the change in the resistivity of the sensor via charge transfer between gas molecules- and diffusivity with Na doped ZnO/PANI rather than Ethanol, CO, Methanol & LPG gas molecules.

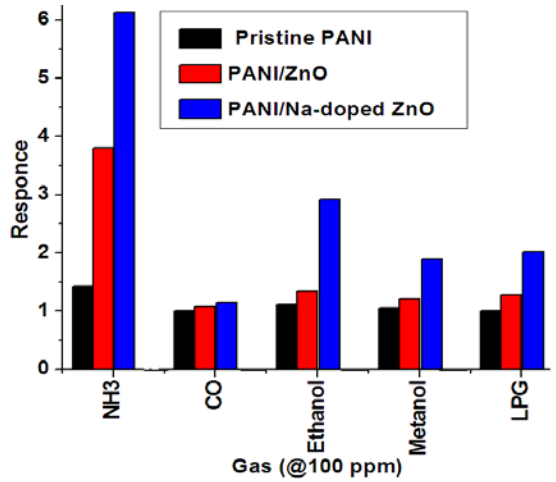

Figure 9. Selectivity of the all samples toward various gases.

Gas-sensing mechanism

The gas sensing mechanism of PANI-ZNO hybrid nanocomposite sensor systematically investigate in the terms of the formation of heterojunctions due to existence *p*-type and *n*-type materials. It can be discussed ZnO nanostructures based sensing materials; the mechanism can be explained by the space-charge layer mode(Sa'aedi &. Yousefi, 2017). In fact, following reaction can be happened when ammonia gas diffuses in PANI layer and reaches to ZnO NWs surface:

$$O_2+e^-_{ZnO\ surface} \rightarrow O^-_{2(ads)} \quad (2)$$

$$NH_3+3O^-_{2(ads)} \rightarrow 2N_2+6H_2O+6e^- \quad (3)$$

It well known that, the resistance of the PANI-ZnO hybrid nanocomposite sensor increases on exposure of NH_3 (electron donor) gas. The protonation and deprotonation process of PANI/ZnO plays essential role in the enhancement of the gas sensing performance. After exposure to NH_3 gas, emeraldine salt form of PANI was reduced to emeraldine base (Das & Sarkar, 2017), resulting into decrease in hole density in PANI, which causes increase in resistance.This can be explained in terms of an energy band diagram of PANI-ZNO hybrid nanocomposite as shown in Figs. 10. Grains of semiconductor metal oxide ZnO are covered with adsorbed oxygen (O_2) molecules, which capture electrons from the conduction band of the ZnO and chemisorbed oxygen species were produced that results in the formation of depletion layer on the surface region of the grains. In PANI/ZNO layer nanocomposite, n-type ZnO NWs form a depletion layer with p-type PANI matrix. When the sensor was exposed to NH_3 gas molecules, the width of depletion layer increases resulting into increase in resistance and hence decreases in conductivity of the sensing material. The adsorption of NH_3 gas molecules in PANI matrix increases space charge region and the modulation in the space charge region at the interface of heterojunction leads to enhance gas sensing performance of PANI-ZnO layer nanocomposite sensor film. In fact, improve electron-donating characteristics is due to formation of p-n heterojunction that could be caused improve the activation energy and enthalpy of physisorption for vapors (Kulkarni et al., 2017). Such conditions affect highly sensitive to the surrounding gaseous environment and local charge carrier concentration could be affected manipulate.

Furthermore, the XPS results indicated that the protonation level of Na doped ZnO is high than all of the other samples.Such improvement of protonation level forNa doped ZnO/PANI sensor could be improved the interaction between N^+–H sites of PANI and ammonia, whichcould be resulted to enhance the sensing properties of heterostructures. Next factor which we think is effective in improvement of gas sensing response of Na doped ZnO/PANI device, is decreasingof nanowire size leading to increasing in surface to volume ratio causes higher diffusion in our device.

Conclusions

PANI/ZnO NWs and PANI/Na-doped ZnO nanowires were used as ammonia gas sensor device at room temperature successfully. The NWs were grown on Si/SiO_2 substrates by a thermal evaporation method and then the PANI layer deposited on the

NWs film by a spin-coating method. Gas sensing measurements indicated that, the devices could work at room temperature to sense ammonia. However, PANI/Na-doped ZnO NWs showed significant operational parameters in compared to the other samples in gas sensing measurements process. So, this can be used to make efficient and low power consumption biosensors. It was discussed that, the protonation and deprotonation process of PANI/ZnO and increasing of surface to volume ratio plays important role in the improvements of the gas sensing performance of PANI/Na-doped ZnO NWs.

Acknowledgment

R. Yousefi would like to acknowledge Islamic Azad University (I.A.U), Masjed-Soleiman Branch for its supporting grant in this research work.

References

A. Sa´aedi, R. Yousefi, F. Jamali-Sheini, M. Cheraghizade, A. Khorsand-Zak, N. M. Huang, Optical properties of group-I-doped ZnO nanowires, Ceramics International. 40 (2014) 4327–4332.

A. Sa'aedi, R. Yousefi, Improvement of gas-sensing performance of ZnOnanorods by group-I elements doping, Journal of Applied Physics. 122 (2017) 224505.

C. Steffens, M.L. Corazza, E. Franceschi, F. Castilhos, P.S. Herrmann, J.V. Oliveira, Development of gas sensors coatings by polyaniline using pressurized fluid, Sens. Actuators. B. 171 (2012) 627-633.

D. D. Nguyen, D. V. Dang and D. C. Nguyen, Advances in Natural Sciences: Nanoscience and Nanotechnology, Hydrothermal synthesis and NH3 gas sensing property of WO3 nanorods at low temperature, 6, (2015) 35.

D.K. Bandgar, S.T. Navale, Y.H. Navale, S.M. Ingole, F.J. Stadler, N. Ramgir, D.K. Aswal, S.K. Gupta, R.S. Mane, V.B. Patil, Flexible camphor sulfonic acid-doped PAni/α-Fe2O3 nanocomposite films and their room temperature ammonia sensing activity, Materials Chemistry and Physics 189 (2017) 191-197.

D.S. Dhawale, D.P. Dubal, A.M. More, T.P. Gujar, C.D. Lokhande, Room temperature liquefied petroleum gas (LPG) sensor, Sensors and Actuators B.147 (2010) 488–494

G. Gaikwad, P. Patil, D. Patil, J. Naik, Synthesis and evaluation of gas sensing properties of PANI based graphene oxide nanocomposites, Materials Science and Engineering B. 218 (2017) 14–22.

G. Zhu, Q. Zhang, G. Xie, Y. Su, K. Zhao, H. Du, Y. Jiang, Gas sensors based on polyaniline/ zinc oxide hybrid film for ammonia detection at room temperature ,Chemical Physics Letters 665 (2016) 147–152.

G.D. Khuspea, D.K. Bandgara, Shashwati Sen, V.B. Patil, Ammonia gas sensing properties of CSA doped PANi-SnO2nanohybridthin films, Synthetic Metals. 185– 186 (2013) 1– 8.

G.Y. Huang, C-Y. Wang, J.T. Wang, First-principles study of diffusion of Li, Na, K and Ag in ZnO, J. Phys: Condens. Matter, 21, 345802 (2009).

H. Tai, Y. Jiang, G. Xie, J. Yu, X. Chen, Z. Ying, Influence of polymerization temperature on NH3 response of PANI/TiO2 thin film gas sensor, Sens. Actuators. B. 129, 319-326 (2008).

H. Tian, W. Wang, Y. Zhu, L. Liao, X. Wang, J. Wang, W. Hu, High performance top-gated ferroelectric field effect transistors based on two-dimensional ZnOnanosheets , Appl. Phys. Lett. 110 (2017) 043505.

H. Xu, D. Ju, W. Li, H. Gong, J. Zhang, J. Wang, B. Cao, Low-working-temperature, fast-response-speed NO2sensor withnanoporous-SnO2/polyaniline double-layered film, Sensors and Actuators B224 (2016) 654–660.

H. Y. Hwang, Y. Iwasa, M. Kawasaki, B. Keimer, N. Nagaosa and Y. Tokura, Emergent Phenomena at Oxide Interfaces, Nature Meter. 11 (2012) 103-113.

L. Geng, Y. Zhao, X. Huang, S. Wang, S. Zhang, S. Wu, Characterization and gas sensitivity study of polyaniline/SnO2 hybrid material prepared by hydrothermal route, Sens. Actuators. B 120 (2007) 568–572.

M. Das, D. Sarkar, One-pot synthesis of zinc oxide - polyanilinenanocomposite for fabrication of efficient room temperature ammonia gas sensor, Ceramics International .40 (2017)11123-11131.

P.P. Sengupta, P. Kar, B. Adhikari, Influence of dopant in the synthesis, characteristics and ammonia sensing behavior of processablepolyaniline, Thin Solid Films 517 (2009) 3770–3775.

S. Bai, Y. Tian, M. Cui, J. Sun, Y. Tian, R. Luo, A. Chen, D. Li, Preparation of conducting films based on α-MoO3/PANI hybrids andtheir sensing properties to triethylamine at room temperature, Sensors and Actuators B 239 (2017) 131–138.

S.B. Kulkarni, Y.H. Navale, S.T. Navale, N.S. Ramgir, A.K. Debnath, S.C. Gadkari, S.K. Gupta, D.K. Aswal, V.B. Patil, Enhanced ammonia sensing characteristics of tungsten oxide decorated polyaniline hybrid nanocomposites, Organic Electronics 45 (2017) 65e73.

S.L. Patil, M.A. Chougule, S. Sen, V.B. Patil , Measurements on room temperature gas sensing properties of CSA doped polyaniline –ZnO nanocomposites, Measurement 45 (2012) 243–249.

V. Talwar, O. Singh, R. C. Singh, ZnO assisted polyaniline nanofibers and its application as ammonia gas sensor, Sensors and Actuators B. 191 (2014) 276– 282.

Y. l. Wang, J. Liu, X. Cui, Y. Gao, J. Ma, Y. Sun, P. Sun, F. Liu, X. Liang, T. Zhang and G. Lu, Sensors and Actuators B: Chemical, NH3 gas sensing performance enhanced by Pt-loaded on mesoporous WO3, 473-481, (2017) 238.

Y. Zhou, Y. Jiang, G. Xie, X. Du, H. Tai, Gas sensors based on multiple-walled carbon nanotubes-polyethylene oxide films for toluene vapor detection, Sensors and Actuators B.191 (2014) 24– 30.

Z. Tong, Y. Yang, J. Wang, J. Zhao, B.L. Su, Y. Li, Layered polyaniline/graphene film from sandwich-structured polyaniline/graphene/polyaniline nanosheets for high-performance pseudo supercapacitors, J. Mater. Chem. A, 2 (2014) 4642-4651.